Blast Wave Reflection Trajectories from a Height of Burst

T.C.J. Hu* and I. I. Glass†
University of Toronto, Toronto, Canada

Consideration is given to an explosive charge (TNT) detonated at various heights of burst above a perfect reflecting planar surface in air. Variations of the incident shock Mach number M_s of the spherical blast wave front as it decays and the corresponding wedge angle θ_w are plotted on a two-dimensional shock wave reflection transition map in the (M_s, θ_w) plane. It is shown that all four types of shock wave reflection (regular, single Mach, complex Mach, and double Mach) can occur in a free-air explosion. However, if the height of burst is increased past a certain limit, only two types of shock wave reflection can occur (regular and single Mach).

Nomenclature

A	= intersection point of the transition lines on the (M_s, θ_w) plane
CMR	= complex Mach reflection
DMR	= double Mach reflection
h	= distance between charge center and ground (HOB)
HOB	= height of burst
I	= incident shock wave
K	= kink
M,M'	= first and second Mach stems
MR	= Mach reflection
M_s	= incident shock wave Mach number
P	= ambient static pressure in the quiescent gas ahead of the blast wave
P_0	= standard atmospheric static pressure
r	= radial distance of the blast wave front from the charge center
r_M	= radial distance between zero ground range and first triple point
R,R'	= first and second reflected shock waves
RR	= regular reflection
S,S'	= first and second slipstreams
SMR	= single Mach reflection
T,T'	= first and second triple points
W	= mass of a TNT charge, kg
W_0	= standard TNT mass of 1 kg
x,x'	= ground range for the RR and MR cases
Y_T	= height of the first triple point
γ	= specific heats ratio
ΔP	= peak overpressure of a blast wave front
Δx	= length of ground distance where a type of reflection occurs
θ_d	= transition angle between RR and MR according to the detachment criterion
θ_w	= wedge angle
χ,χ'	= first and second triple-point trajectory angles
$\leftrightarrow$	= transition between two types of reflections

Received Feb. 5, 1985; revision received June 12, 1985.

*Research Assistant, Institute for Aerospace Studies. Student Member AIAA.

†University Professor, Institute for Aerospace Studies. Fellow AIAA.

Introduction

With the knowledge of blast wave flows and oblique shock wave reflections gained in recent years,[1-6] it is now possible to trace the path of a spherical blast wave detonated in free air on a transition map in the (M_s, θ_w) plane. In an explosion, the flowfield near the charge is very complex and very difficult to analyze. However, when the blast wave front outruns the fireball and starts to interact with the ground surface, the flow can be reasonably assumed to be two-dimensional at any instant of time. Hence, the analysis used here for pseudostationary flow can be applied to the interaction of a blast wave with a planar surface. It becomes possible to predict the type of reflection, the incident shock Mach number, and the corresponding wedge angle that a target at a known distance away from the explosion may encounter. This predictive information is of great value to researchers and experimenters in the field.

The four types of pseudostationary oblique shock wave reflection patterns observed in air are shown schematically in Fig. 1. The figure illustrates the definition of various shock waves I, R, R', M, and M', slipstreams S and S', triple points T and T', kink K, triple-point trajectory angles χ and χ', wedge angle θ_w, and the flow regions (1) to (5) produced by the four reflections.

The flowfield associated with a free-air explosion is shown in Fig. 2. To demonstrate how the study of oblique shock wave reflection can be applied to the interaction of a spherical blast wave with a planar surface, consideration is given to a typical charge of TNT detonated in free air followed by the blast wave reflection from a perfect planar surface in a standard atmosphere of 101 kPa and 288 K. The TNT explosion data used in this study come from a combination of surface hemispherical burst and free-air spherical burst results. Actually, they are two different types of explosions. However, if the free-air spherical bursts are scaled to surface hemispherical bursts by using Sachs's scaling law[7] with a factor of exactly two, the surface and free-air data collapse under scaled form to a fairly consistent set of results,[8] giving better agreement especially for $\Delta P > \frac{1}{3}$ atm (33.8 kPa) or $M_s > 1.15$. A curve is then fitted through the data to obtain an equation that relates to ΔP as a function of r.

For a given HOB h, the ground range x and the corresponding wedge angle θ_w are related geometrically to the radial distance r in the case of RR. However, in the case of MR, the computation of the ground range x and the corresponding wedge angle θ_w are complicated by the introduction of the first

triple-point trajectory. Since the Mach stem M is usually bulged out in real explosions or large-scale field tests, the ground range x is simply estimated by assuming that the Mach stem M is an arc of a circle with the radius being the distance between zero ground range and the first triple-point T, which is shown as r_M in Fig. 2b.

Since the spherical blast wave flow can be treated as two-dimensional at any instant of time, the merging of the two triple points at the RR↔DMR transition boundary applies and there exists a blast wave trajectory path that crosses point A, where all three transition lines meet on the transition map (Fig. 3). For a critical assessment of the transition lines, the reader is referred to Refs. 4 and 6.

Algorithm

An equation is obtained by curve fitting the surface burst and free-air burst data in a scaled form.[9] It is in good agreement with the data from Sadek and Gottlieb[10] and Dewey.[11] It gives slightly higher values than the data from Brode[12] and fits best with the data from Baker.[13] The curve fit equation provides $\Delta P/P_0$ as a function of r. The blast wave front M_s can then be calculated from ΔP using one of the Rankine-Hugoniot equations

$$\Delta P = \frac{2\gamma}{\gamma+1}(M_s^2 - 1) \tag{1}$$

where the air is assumed to be a perfect gas with $\gamma = 7/5$.

In the calculation of the blast wave front trajectory path of the (M_s, θ_w) transition map, a HOB h is first chosen. The blast wave front overpressure ΔP is determined from the curve fit equation for a given r. The blast wave front M_s is then calculated from Eq. (1).

For RR, at a given HOB h and r, M_s can be calculated as mentioned above. The ground range x and the corresponding wedge angle θ_w, as shown in Fig. 2a, can be determined from the relations

$$x^2 = r^2 - h^2 \tag{2}$$

$$\sin\theta_w = h/r \tag{3}$$

For MR, at a given HOB h and r, M_s is calculated the same way as for RR. To find the ground range x and the wedge angle θ_w, it is essential to know the height of the first triple point Y_T. As illustrated in Fig. 2b, x, h, Y_T, and θ_w are related by

$$r^2 = x^2 + (h - Y_T)^2 \tag{4}$$

$$\tan\theta_w = (h - Y_T)/x \tag{5}$$

and the slope of the first triple-point trajectory is given by

$$dY_T/dx = \tan\chi \tag{6}$$

If Eq. (5) is first differentiated, then substituted into Eq. (6), and the result integrated, the following two relations are obtained[14]:

$$Y_T/h = 0 \qquad \text{for } \theta_w > \theta_d \tag{7}$$

$$\frac{Y_T}{h} = 1 - \exp\int_{\theta_d}^{\theta_w} \frac{\tan\chi\, d\theta_w}{\sin^2\theta_w(1 + \tan\chi/\tan\theta_w)} \qquad \text{for } \theta_w < \theta_d \tag{8}$$

where θ_d is RR↔MR transition angle according to the detachment criterion.[15] Equation (7) is applicable to RR stating that no triple point exists if θ_w is above θ_d. Equation (8) is applicable to MR and can be integrated if the relation between θ_w and χ in a two-dimensional shock tube flow is assumed valid.

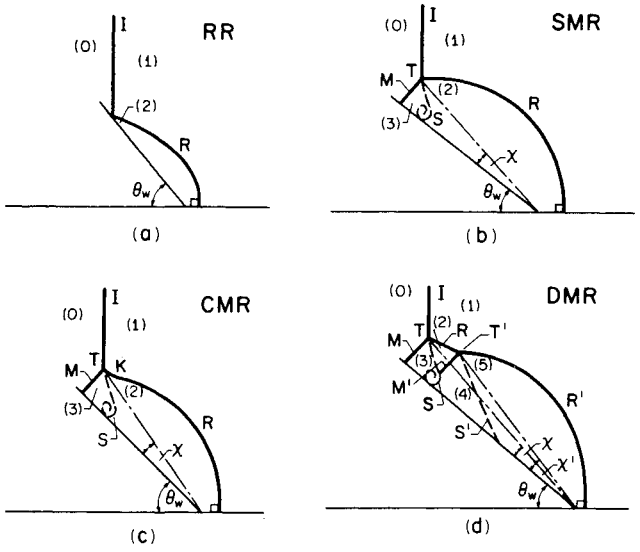

Fig. 1 Four basic types of oblique shock-wave reflections: a) RR, b) SMR, c) CMR, and d) DMR.

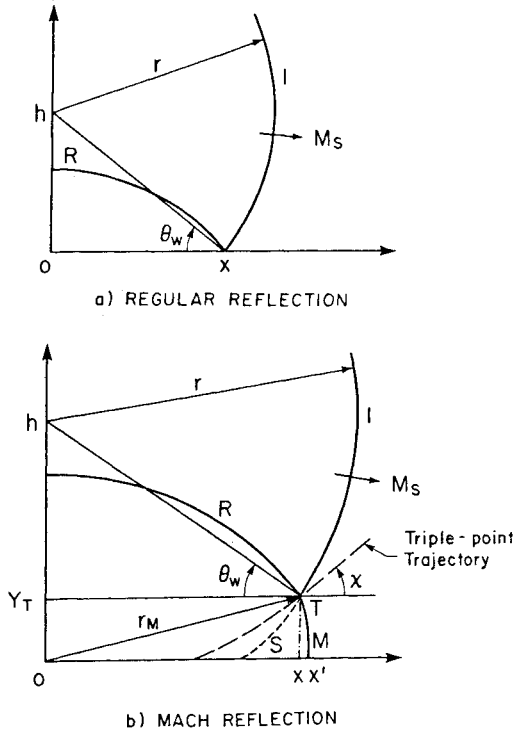

Fig. 2 Flowfield of a free-air explosion.

The following fixed-point iterative scheme is used to determine the value of Y_T:

1) The HOB h and r are given.
2) Calculate M_s for a given r.
3) An initial guess is made of Y_T.
4) Calculate the wedge angle θ_w from the relation obtained by substituting Eq. (4) into Eq. (5),

$$\theta_w = \tan^{-1}\left\{\left[\frac{r^2}{(h - Y_T)^2} - 1\right]^{-1/2}\right\} \tag{9}$$

5) With θ_w, calculate Y_T using Eq. (8).
6) Check if $|(Y_T^{new} - Y_T^{old})/Y_T^{old}| \le 10^{-5}$.
7) Steps 4 and 5 are repeated until the tolerance in step 6 is achieved.

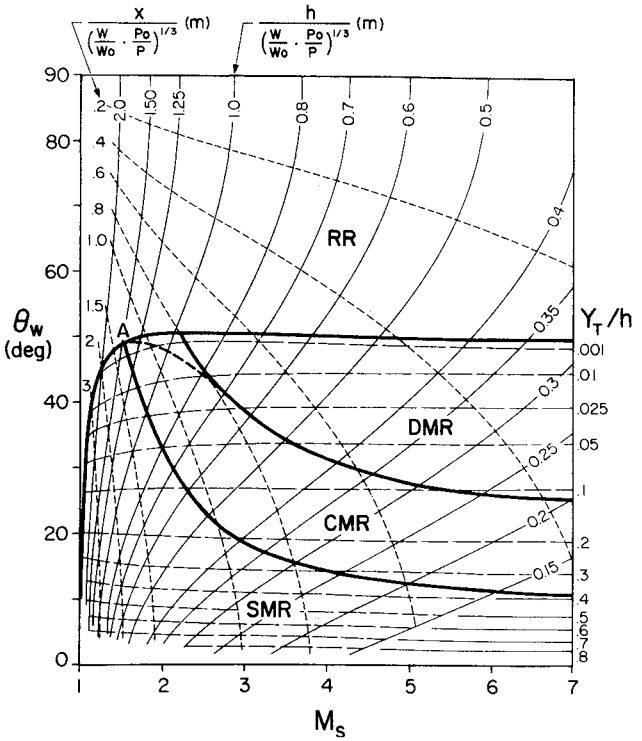

Fig. 3 Interaction of a spherical blast wave with a planar surface in perfect air at standard ambient conditions.

Once Y_T is determined, x and θ_w can be calculated using Eqs. (4) and (5). In real explosions, the Mach stem M is not entirely straight from the first triple point to the ground, but curved as shown in Fig. 2b. Such a bulging effect of the Mach stem is simply simulated by assuming that M is an arc cutting the first triple point at T and the ground at x' with its radius being r_M. The ground range x in MR then takes the value of x'.

Results and Discussion

The computed results of the blast wave front trajectory path for various HOB cases are presented graphically in Fig. 3 on a transition map in the (M_s, θ_w) plane. Contours of ground range x and height of the first triple point Y_T are also plotted. The height of burst h and ground range x in the figure are scaled to the weight of the charge W and the ambient pressure P by introducing a nondimensionalized scaling factor[10] of $(W/W_0 \cdot P_0/P)^{-1/3}$, where W_0 and P_0 are taken as 1 kg and 1 atm, respectively. The height of the first triple point Y_T is also shown as a fraction of the HOB h.

Assume that a charge of 1 kg TNT is detonated at a HOB of 0.5 m with an ambient pressure of 1 atm. When the blast wave front just hits the planar surface directly under the charge, $x=0$ m, $\theta_w=90$ deg, and $M_s=6.0$. As the blast wave front propagates outward, the incident shock wave collides with and is reflected off the planar surface, resulting in regular reflection RR, which occurs up to a ground range of $x=0.41$ m. At the same time, M_s diminishes to 4.6. When DMR just occurs, the height of the first triple point Y_T is zero at the transition line and DMR continues in the range of $0.41\text{ m}<x<0.70$ m. At the transition point from DMR to CMR, M_s decreases to 3.5, Y_T increases to 0.048 m, and CMR occurs in the ground range of $0.70\text{ m}<x<1.04$ m. At the termination of CMR, M_s drops to 2.6, Y_T grows to almost 0.16 m, and SMR begins to form at a ground range of $x>1.04$ m.

With a given charge weight W, ambient pressure P, HOB h, and ground range x, one can read from Fig. 3 M_s, θ_w, Y_T, and the type of reflection that is going to occur. With M_s and θ_w, the flow properties behind the blast wave front at the ground range x can be predicted using the numerical results presented in tabular and graphical forms by Hu and Shirouzu.[16] These results are essential in predicting the dynamic response of structures in the vicinity of a blast wave. For a different explosive charge and height of burst, a different blast wave front path has to be constructed on the transition map in order to predict what type of reflection would occur for a certain ground range. Figure 3 also shows the effect of changing the height of burst and charge weight on the blast wave front trajectory path. The trajectories of 14 different HOB cases are calculated and plotted on the same figure to show the effect of changing the HOB.

There are several interesting points that can be made about Fig. 3:

1) Increasing the HOB for a given charge will decrease the incident shock wave Mach number M_s of the blast wave as it interacts with the planar surface.

2) Let Δx be defined as the difference between the ground range where a specific type of reflection begins and where it terminates. For example, on the scaled line $h=0.5$ m, x increases from 0 m for $\theta_w=90$ deg to 0.41 m when $\theta_w\simeq 50$ deg at the RR↔DMR line and $\Delta x=0.41$ m. In RR region, Δx increases with HOB. For example, at a scaled h of 0.5, $\Delta x=0.41$ m; at $h=0.7$ m, $\Delta x=0.58$ m; at $h=1.0$ m, $\Delta x=0.81$ m; and at $h=2.0$ m, $\Delta x=1.95$ m. However, in both DMR and CMR regions, there is a HOB h that gives an optimum Δx. This is because at small h, Δx increases with HOB. As h becomes large, the domains of both DMR and CMR diminish and thus their Δx also decrease. For instance, in the DMR region, at a scaled h of 0.3 m, $\Delta x=(0.53-0.25)=0.28$ m; at $h=0.35$ m, $\Delta x=(0.58-0.29)=0.29$ m; at $h=0.4$ m, $\Delta x=(0.63-0.33)=0.30$ m; at $h=0.5$ m, $\Delta x=(0.70-0.41)=0.29$ m; and at $h=0.6$, $\Delta x=(0.76-0.50)=0.26$ m. Due to the increasing and decreasing behavior of Δx, a maximum Δx exists in the DMR domain; this also applies to the CMR domain. In the SMR region, Δx is an increasing function of HOB, since the SMR domain enlarges at low M_s.

3) Theoretically, the interaction of a blast wave front with the ground may result in three possible series of reflections: RR→DMR→CMR→SMR, RR→CMR→SMR, or RR→SMR. However, experiments have shown that the CMR↔DMR transition line approaches the SMR↔CMR transition line and merges at a single point A on the RR termination boundary as shown by the heavy dash line in Fig. 3. Therefore, only two possible series of reflection can occur: RR→DMR→CMR→SMR or RR→SMR. The latter occurs if $h/(W/W_0 \cdot P_0/P)^{-1/3} \geq 1.5$ m.

4) From Fig. 3, it can be seen that owing to the steepness of the RR↔SMR transition line compared to the blast wave paths in the (M_s, θ_w) plane, RR cannot reoccur when $M_s \to 1$.

5) Increasing the charge weight W has the same effect as decreasing the HOB or increasing M_s, whereas an increase in the ambient pressure P has results similar to increasing the HOB or decreasing M_s.

Conclusions

A method to study the interaction of a blast wave with a planar surface is presented. It is used in predicting the trajectory path of the blast wave front for the HOB case on the transition map of pseudostationary oblique shock wave reflection and providing information on the instantaneous type of reflection, wedge angle, blast wave front Mach number, ground range, and height of the first triple point as the blast wave propagates. With M_s and θ_w being known at any point along the trajectory path of a blast wave front, the corresponding reflection flow properties can be obtained from tables and graphs.[16] The method and results presented here are the first of their kind. Although TNT was chosen as the explosive to be studied, the method can be used to obtain similar results for other types of explosives.

For a spherical flow, the growth of the reflected spherical shocks R and R' cannot be determined from a two-dimensional analysis. Consequently, the second triple-point T' trajectory is indeterminate using this analysis. It would be important to verify the present results experimentally in field tests. If reasonable agreement is obtained, then it has been shown that the blast wave interaction with a planar surface can be analyzed by this rather simplified method. It would also be of interest to perform the same analysis with real-gas effects included and to compare the results with field test data to determine which model gives between agreement.

Acknowledgment

We wish to thank Dr. J. J. Gottlieb for his assistance and technical advice during the course of this work. The financial assistance received from the Canadian Natural Sciences and Engineering Research Council, the U.S. Air Force under grant AF-AFOSR 82-0096, and the U.S. Defense Nuclear Agency under DNA Contract 001-83-C-0266 is gratefully acknowledged.

References

[1]Ben-Dor, G. and Glass, I. I., "Domains and Boundaries of Nonstationary Oblique Shock-Wave Reflection: I. Diatomic Gas," *Journal of Fluid Mechanics*, Vol. 92, Pt. 3, June 1979, pp. 459-496.

[2]Ben-Dor, G. and Glass, I. I., "Domains and Boundaries of Nonstationary Oblique Shock-Wave Reflections: II. Monatomic Gas," *Journal of Fluid Mechancis*, Vol. 96, Pt. 4, Feb. 1980, pp. 735-756.

[3]Ando, S. and Glass, I. I., "Domains and Boundaries of Pseudostationary Oblique-Shock-Wave Reflections on Carbon Dioxide," *Proceedings of the 7th International Symposium on the Military Applications of Blast Simulation*, Defence Research Establishment Suffield, Ralston, Canada, 1981.

[4]Shirouzu, M. and Glass, I. I., "Assessment of Recent Results on Pseudo-Stationary Oblique-Shock-Wave Reflections," University of Toronto, Institute for Aerospace Studies, Rept. 264, Nov. 1982.

[5]Lee, J.-H. and Glass, I. I., "Pseudo-Stationary Oblique-Shock-Wave Reflections in Frozen and Equilibrium Air," *Progress in Aerospace Sciences*, Vol. 21, No. 1, 1984, pp. 33-80.

[6]Hu, T. C. J. and Glass, I. I., "Pseudostationary Oblique-Shock-Wave Reflections in Sulfur Hexafluoride (SF_6): Interferometric and Numerical Results," submitted to the Proceedings of the Royal Society of London.

[7]Sachs, R. G., "The Dependence of Blast on Ambient Pressure and Temperature," U.S. Army Ballistic Research Laboratory, Aberdeen Proving Ground, MD, BRL Rept. 446, 1944.

[8]"Structures to Resist the Effects of Accidental Explosions," U.S. Dept. of the Army Technical Manual TM 5-1300, Dept. of the Navy Publication NAVFAC P-397, Dept. of the Air Force Manual AFM 88-22, June 1969.

[9]Gottlieb, J. J., Private communication on HOB Curve-Fit Equation, 1985.

[10]Sadek, H. S. and Gottlieb, J. J., "Initial Decay of Flow Properties of Planar, Cylindrical and Spherical Blast Waves," University of Toronto, Institute for Aerospace Studies, Tech. Note 244, Oct. 1983.

[11]Dewey, J. M., "The Air Velocity and Density in Blast Waves from TNT Explosions," Defence Research Establishment Suffield, Ralston, Canada, DRES Rept. 207, March 1964.

[12]Brode, H. L., "A Calculation of the Blast Wave from a Spherical Charge of TNT," Rand Corp., Santa Monica, CA, Rept. RM-1965, 1957.

[13]Baker, W. E., *Explosions in Air*, University of Texas Press, Austin, TX, 1973.

[14]Mirels, H., "Mach Reflection Flow Fields Associated with Strong Shocks," Space Division, U.S. Air Force Systems Command, Rept. SD-TR-83-50, July 1983.

[15]von Neumann, J., "Oblique Reflection of Shocks," U.S. Department of the Navy, Bureau of Ordance, Explosives Research, Rept. 12, Oct. 1943.

[16]Hu, T. C. J. and Shirouzu, M., "Tabular and Graphical Solutions of Regular and Mach Reflections in Pseudo-Stationary Frozen and Vibrational-Equilibrium Flows," University of Toronto, Institute for Aerospace Studies, Rept. 283, June 1985.